



ELSEVIER

Contents lists available at ScienceDirect

## Comptes Rendus Physique

www.sciencedirect.com



Probing matter with electromagnetic waves / Sonder la matière par les ondes électromagnétiques

## Combined complex-source beam and spherical-multipole analysis for the electromagnetic probing of conical structures



*Combinaison de faisceaux de sources complexes et décomposition en modes sphériques pour le sondage électromagnétique des structures coniques*

Ludger Klinkenbusch\*, Hendrik Brüns

Kiel University, Kaiserstr. 2, 24143 Kiel, Germany

## ARTICLE INFO

## Article history:

Available online 12 August 2016

## Keywords:

Complex-source beam  
Spherical-multipole analysis  
Conical structures  
Green's functions  
Radiation condition

## Mots-clés:

Faisceau source complexe  
Analyse multipôle sphérique  
Structure conique  
Fonction de Green  
Condition de radiation

## ABSTRACT

The paper addresses the combination of the spherical-multipole analysis in sphero-conal coordinates with a uniform complex-source beam (CSB) in order to analyze the scattering of a localized electromagnetic plane wave by any desired part of a perfectly conducting elliptic cone. The concept of uniform CSB is introduced and rigorously applied to the diffraction by a semi-infinite elliptic cone. The analysis takes into account the fact that the incident CSB does not satisfy the radiation condition. A new modal form of the Green's function for the elliptic cone is derived based on the principle that there is no energy loss to infinity. The numerical evaluation includes the scattered far fields of a CSB incident on the corner of a plane angular sector with different opening angles.

© 2016 Académie des sciences. Published by Elsevier Masson SAS. All rights reserved.

## R É S U M É

Cet article présente la combinaison de l'analyse de multipôles sphériques en coordonnées sphéro-coniques avec une faisceau de source complexe (*Complex Source Beam*, CSB) dans le but d'analyser la diffusion localisée par un cône elliptique parfaitement conducteur d'une onde plane électromagnétique. Le concept de CSB est introduit au travers de la diffraction par un cône elliptique semi-infini. L'analyse prend en compte le fait que l'onde CSB incidente ne satisfait pas les conditions de radiation. Un nouveau modèle de la fonction de Green pour un cône elliptique est développé en faisant l'hypothèse qu'il n'y a pas de pertes d'énergie à l'infini. Le modèle numérique inclut la diffusion en champ lointain d'une source CSB sur le coin d'un secteur angulaire avec différents angles d'ouverture.

© 2016 Académie des sciences. Published by Elsevier Masson SAS. All rights reserved.

\* Tel.: +49 431 8806252; fax: +49 431 8806253.

E-mail address: [lbk@tf.uni-kiel.de](mailto:lbk@tf.uni-kiel.de) (L. Klinkenbusch).

## 1. Introduction

Multipole analysis and complex-source beams (CSB) are important techniques in field theory. As examples for applications, multipole expansions are in use to solve and compactly characterize scalar, electrodynamic, and elastodynamic fields in the presence of canonical structures while complex-source beams are perfectly suited to elegantly produce analytic beam-like fields. With a combination of both methods, it is possible to analytically investigate the scattering and diffraction of a beam-like electromagnetic wave by canonical structures. Particularly, the elliptic cone which is described as a coordinate surface in sphero-conal coordinates contains several interesting special cases, including the half plane, the quarter plane, and the circular cone. The corresponding electromagnetic boundary-value problem is solved via the dyadic Green's function, which consists of bilinear products of spherical Bessel functions, periodic, and non-periodic Lamé functions. With an incident CSB, it is possible to probe any geometrical detail of the structure and thus to isolate the corresponding electromagnetic response. Particularly, the tip and edge diffraction coefficients derived from these solutions can be applied to further complete asymptotic high-frequency methods like the Geometrical Theory of Diffraction (GTD) or the Uniform Theory of Diffraction (UTD) [1].

The paper starts with brief summaries of the spherical-multipole analysis in sphero-conal coordinates and the complex-source beam technique. Then the concept of the uniform CSB is introduced and thoroughly applied to the diffraction by a semi-infinite elliptic cone. The analysis is similar to the derivation of the classical Green's function of the cone, but takes into account the fact that the uniform CSB does not satisfy the radiation condition. The numerical evaluation includes the scattered far fields of a uniform CSB incident on the corner of a plane angular sector with different opening angles.

## 2. Spherical-multipole analysis in sphero-conal coordinates

Sphero-conal (conical) coordinates  $r, \vartheta, \varphi$  are related to Cartesian coordinates by

$$x = r \sin \vartheta \cos \varphi \quad (1)$$

$$y = r \sqrt{1 - k^2 \cos^2 \vartheta} \sin \varphi \quad (2)$$

$$z = r \cos \vartheta \sqrt{1 - k'^2 \sin^2 \varphi} \quad (3)$$

They belong to those famous eleven three-dimensional coordinate systems where the Helmholtz equation is fully separable [2].  $k$  and  $k'$  are positive real-valued parameters which satisfy  $k^2 + k'^2 = 1$ . The coordinate surface  $\vartheta = \vartheta_0$  generally describes a semi-infinite elliptic cone where the degree of ellipticity is defined by the choice of  $k$ . In the case where  $k = 1$ , the sphero-conal coordinates turn into regular spherical coordinates, and the elliptic cone becomes a right-circular cone. In the case where  $\vartheta_0 = 0$  or  $\vartheta_0 = \pi$ , the elliptic cone degenerates to a plane angular sector in the  $yz$ -plane symmetrically around the  $+z$  and  $-z$  axis, respectively, with an opening angle defined by  $2 \arccos(k)$ . We denote the normalized metric scaling coefficients by

$$s_{\vartheta} = \frac{1}{r} \left| \frac{\partial \mathbf{r}}{\partial \vartheta} \right| = \sqrt{\frac{k^2 \sin^2 \vartheta + k'^2 \cos^2 \varphi}{1 - k^2 \cos^2 \vartheta}} \quad (4)$$

$$s_{\varphi} = \frac{1}{r} \left| \frac{\partial \mathbf{r}}{\partial \varphi} \right| = \sqrt{\frac{k^2 \sin^2 \vartheta + k'^2 \cos^2 \varphi}{1 - k'^2 \sin^2 \varphi}} \quad (5)$$

The scalar homogeneous Helmholtz equation reads in sphero-conal coordinates

$$\begin{aligned} \Delta \Phi_{\sigma}(\mathbf{r}) + \kappa^2 \Phi_{\sigma}(\mathbf{r}) &= 0 \\ \frac{1}{r^2} \frac{\partial}{\partial r} \left( r^2 \frac{\partial \Phi_{\sigma}(\mathbf{r})}{\partial r} \right) + \frac{1}{r^2} (\mathbf{r} \times \nabla)^2 \Phi_{\sigma}(\mathbf{r}) + \kappa^2 \Phi_{\sigma}(\mathbf{r}) &= 0 \end{aligned} \quad (6)$$

where the angular part of the  $\Delta$ -operator is related to the square of the angular-momentum operator known from quantum mechanics and defined by [3]:

$$(\mathbf{r} \times \nabla)^2 = \frac{s_{\vartheta}}{s_{\varphi}} \left[ \frac{\partial}{\partial \vartheta} \left( \frac{s_{\varphi}}{s_{\vartheta}} \frac{\partial}{\partial \vartheta} \right) + \frac{\partial}{\partial \varphi} \left( \frac{s_{\vartheta}}{s_{\varphi}} \frac{\partial}{\partial \varphi} \right) \right] \quad (7)$$

The method of separation of variables yields an elementary solution of (6) according to

$$\Phi_{\sigma}(r, \vartheta, \varphi) = z_{\sigma}(\kappa r) \Theta_{\sigma}(\vartheta) \Phi_{\sigma}(\varphi) \quad (8)$$

The separation constants are denoted by  $\sigma$  and  $\lambda$ .  $z_{\sigma}$  is a spherical Bessel function, while  $\Theta_{\sigma}$  and  $\Phi_{\sigma}$  represent non-periodic and periodic Lamé functions, respectively. The products of non-periodic and periodic Lamé functions are referred to as Lamé products  $Y_{\sigma}(\vartheta, \varphi) = \Theta_{\sigma}(\vartheta) \Phi_{\sigma}(\varphi)$ . They satisfy the eigenvalue equation

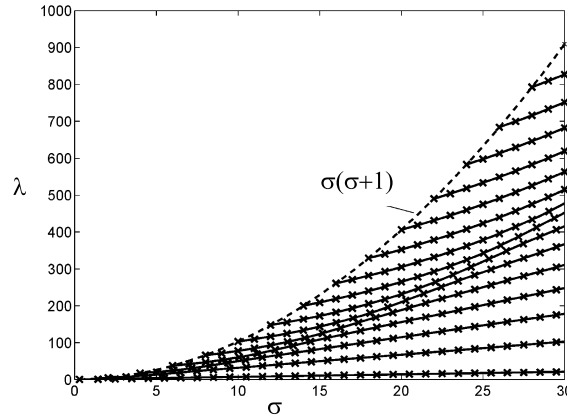


Fig. 1. Eigenvalue curves  $\lambda(\sigma)$  and discrete Dirichlet eigenvalues  $\sigma_s(\times)$  for  $\vartheta_0 = 180^\circ$  and  $k^2 = 0.5$  (quarter plane).

$$(\mathbf{r} \times \nabla)^2 Y_\sigma(\vartheta, \varphi) + \sigma(\sigma + 1)Y_\sigma(\vartheta, \varphi) = 0 \tag{9}$$

It can be shown [3] that for any valid solution of the boundary value problem at hand, the possible discrete values of  $\sigma$  and  $\lambda$  have to lie on the so-called eigenvalue curves, as exemplarily represented in Fig. 1. We are interested in those eigenvalues  $\sigma_s$  satisfying the Dirichlet condition (index  $s$  for acoustically soft) or the Neumann condition ( $\sigma_h$ ; index  $h$  for acoustically hard) at  $\vartheta_0$  according to

$$\Theta_{\sigma_s}(\vartheta_0) = 0 \quad ; \quad \left. \frac{d\Theta_{\sigma_h}}{d\vartheta}(\vartheta) \right|_{\vartheta=\vartheta_0} = 0 \tag{10}$$

respectively. The corresponding discrete pairs of eigenvalues  $(\sigma_\tau, \lambda)$  with  $\tau \in \{s, h\}$  are found by a numerically performed search on the aforementioned eigenvalue curves. Note that the Lamé products satisfying (10) form an orthogonal system of functions on the domain  $0 \leq \vartheta \leq \vartheta_0; 0 \leq \varphi \leq 2\pi$ .

For the solution of the electromagnetic problem, the same spherical-multipole technique as in ordinary spherical coordinates applies. As has been shown in [3] outside of a perfectly electrically conducting (PEC) elliptic cone in a homogeneous, isotropic, and linear medium characterized by permittivity  $\epsilon$  and permeability  $\mu$ , the time-harmonic electromagnetic field at a time factor  $e^{+j\omega t}$  is represented by the spherical-multipole expansion

$$\begin{aligned} \mathbf{E}(\mathbf{r}) &= \sum_{\sigma_s} a_{\sigma_s} \mathbf{N}_{\sigma_s}(\mathbf{r}) + \frac{Z}{j} \sum_{\sigma_h} b_{\sigma_h} \mathbf{M}_{\sigma_h}(\mathbf{r}) \\ \mathbf{H}(\mathbf{r}) &= \frac{j}{Z} \sum_{\sigma_s} a_{\sigma_s} \mathbf{M}_{\sigma_s}(\mathbf{r}) + \sum_{\sigma_h} b_{\sigma_h} \mathbf{N}_{\sigma_h}(\mathbf{r}) \end{aligned} \tag{11}$$

Here,  $Z = \sqrt{\mu/\epsilon}$  is the intrinsic impedance of the medium, while the expansion functions, which are also known as vector spherical-multipole functions, are related to the elementary solutions of the scalar homogeneous Helmholtz equation by

$$\mathbf{M}_{\sigma_\tau}(\mathbf{r}) = (\mathbf{r} \times \nabla) \Phi_{\sigma_\tau}(\mathbf{r}) \quad ; \quad \mathbf{N}_{\sigma_\tau}(\mathbf{r}) = \frac{1}{\kappa} \nabla \times \mathbf{M}_{\sigma_\tau}(\mathbf{r}) \quad (\tau \in s, h) \tag{12}$$

where  $\kappa = \omega\sqrt{\mu\epsilon}$  is the wave number of the medium. The expansion coefficients in (11) are referred to as the spherical-multipole amplitudes  $a_{\sigma_s}$  and  $b_{\sigma_h}$ . They contain the entire information of the total electromagnetic field for a specific source, e.g., a Hertzian dipole.

### 3. Uniform complex-source beam

By assigning a complex-valued location  $\mathbf{r}_c = \mathbf{r}_w - j\mathbf{b}$ , a point source field (e.g., due to a Hertzian dipole) is turned into a complex-source beam (CSB) [4,5]. In a paraxial approximation, that CSB represents a Gaussian beam. In contrast to a Gaussian beam, the CSB is an exact solution of Maxwell’s equations. The location of the beam’s waist is defined by the real part  $\mathbf{r}_w$ , while the direction of beam propagation and the focus (Rayleigh) length is given by the imaginary part  $\mathbf{b}$ . If the original point-source field satisfies the radiation condition (i.e. only outwardly traveling waves are allowed in the far field), that condition is preserved for a complex source location, i.e. all inwardly traveling field parts (towards the waist) of the resulting CSB are exponentially damped and virtually not relevant. On the other hand, if the location of a point sink—with only inwardly traveling waves—is defined as complex-valued, the CSB parts traveling outwardly (from the waist) are exponentially damped. Consequently, by simply adding these two fields, a uniform CSB (a complete CSB) is achieved, which includes an analytic local plane wave at the waist [6].

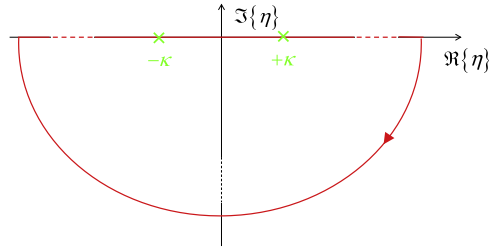


Fig. 2. Path of integration in the complex  $\eta$ -plane for solving (17).

#### 4. Green's function of an elliptic cone illuminated by a uniform complex-source beam

As mentioned above, a uniform CSB does not satisfy the radiation condition. Hence the Green's function for the elliptic cone which usually takes into account that condition has to be re-deduced if the cone is illuminated by a uniform CSB. For the sake of simplicity and because the electromagnetic case is a straightforward extension of the scalar case, we will demonstrate the derivation for a scalar Green's function satisfying

$$\Delta G_s(\mathbf{r}, \mathbf{r}_c) + k^2 G_s(\mathbf{r}, \mathbf{r}_c) = \delta_s(\mathbf{r} - \mathbf{r}_c) \tag{13}$$

subject to the Dirichlet (soft) boundary condition

$$G_s(\mathbf{r}, \mathbf{r}_c)|_{\vartheta=\vartheta_0} = 0 \tag{14}$$

First we express the three-dimensional  $\delta$  distribution by using the corresponding completeness relation according to (see [3] p. 566 for a derivation):

$$\delta_s(\mathbf{r} - \mathbf{r}_c) = \frac{2}{\pi} \int_0^\infty \eta^2 \sum_{\sigma_s} j_{\sigma_s}(\eta r) j_{\sigma_s}(\eta r_c) d\eta Y_{\sigma_s}(\vartheta, \varphi) Y_{\sigma_s}^*(\vartheta_c, \varphi_c) \tag{15}$$

where  $j_{\sigma_s}$  represents the spherical Bessel function of the first kind of order  $\sigma_s$ , and the asterisk denotes the complex conjugation. Next we expand the Green's function by means of the complete bilinear eigenfunction expansion

$$G_s(\mathbf{r}, \mathbf{r}_c) = \frac{2}{\pi} \int_0^\infty \eta^2 \sum_{\sigma_s} a_{\sigma}(\eta) j_{\sigma_s}(\eta r) j_{\sigma_s}(\eta r_c) d\eta Y_{\sigma_s}(\vartheta, \varphi) Y_{\sigma_s}^*(\vartheta_c, \varphi_c) \tag{16}$$

We insert (15) and (16) into (13) and use the eigenvalue equation (9) as well as the orthogonality properties of the Lamé products on the unit sphere and of the spherical Bessel functions on the interval  $[0, \infty)$  to obtain

$$G_s(\mathbf{r}, \mathbf{r}_c) = \frac{2}{\pi} \int_0^\infty \frac{\eta^2}{\kappa^2 - \eta^2} \sum_{\sigma_s} j_{\sigma_s}(\eta r) j_{\sigma_s}(\eta r_c) d\eta Y_{\sigma_s}(\vartheta, \varphi) Y_{\sigma_s}^*(\vartheta_c, \varphi_c) \tag{17}$$

The integral in (17) can be solved similarly to the approach in [7] using residue calculus in the complex  $\eta$ -plane. However, in opposite to [7], where the poles of (17) at  $\eta = \pm\kappa$  have to be properly excluded from the path of integration to satisfy the radiation condition, in the present case of a uniform CSB we have to take in account that there is no energy loss to infinity. Consequently, as shown in Fig. 2, the path of integration has to stay on the real axis to account for that conservation of energy for any  $\eta$ .

For a complex-valued source location  $\mathbf{r}_c = \mathbf{r}_w - \mathbf{j}\mathbf{b}$  where  $\mathbf{r}_w$  and  $\mathbf{b}$  are real and  $\mathbf{b} > 0$ , we finally derive the modal expansion of the Green's function as

$$G_s(\mathbf{r}, \mathbf{r}_c) = 2jk \sum_{\sigma_s} j_{\sigma_s}(\kappa r) j_{\sigma_s}(\kappa r_c) Y_{\sigma_s}(\vartheta, \varphi) Y_{\sigma_s}^*(\vartheta_c, \varphi_c) \tag{18}$$

Note that there is no case distinction  $|r| \geq |r_c|$  as necessary for the Green's function satisfying the radiation condition. Moreover, the expansion (18) is equally convergent for  $|r| = |r_c|$  as well. The acoustic field at  $\mathbf{r}$  due to a point source  $Q$  located at  $\mathbf{r}_c$  in the presence of a acoustically soft elliptic cone can then be represented by  $\Phi(\mathbf{r}) = G_s(\mathbf{r}, \mathbf{r}_c)Q$ .

The extension to the electromagnetic case, i.e. to a dyadic Green's function can be performed as usual [8]. For a Hertzian dipole  $\mathbf{c}_{el}$  located at  $\mathbf{r}_c$ , the electromagnetic field in the presence of an elliptic cone can finally be represented by the spherical-multipole expansion (11) with multipole amplitudes

$$a_{\sigma_s} = -\kappa^2 Z \frac{1}{\sigma_s(\sigma_s + 1)} \mathbf{N}_{\sigma_s}^*(\mathbf{r}_c) \cdot \mathbf{c}_{el} \quad ; \quad b_{\sigma_h} = -j\kappa^2 \frac{1}{\sigma_h(\sigma_h + 1)} \mathbf{M}_{\sigma_h}^*(\mathbf{r}_c) \cdot \mathbf{c}_{el} \tag{19}$$

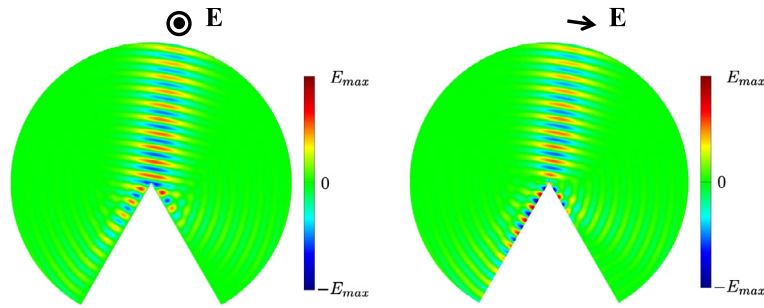


**Fig. 3.** Total field of a uniform CSB incident on the tip of a circular cone. The waist is located directly at the tip. The Rayleigh length is  $b = 10 \Lambda$  ( $\Lambda =$  wavelength). The angle of incidence is  $\theta = 10^\circ$  of the vertical axis. The polarizations are as indicated.

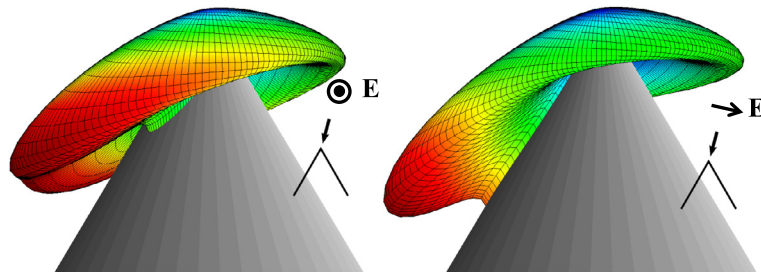


**Fig. 4.** Scattered far field of a uniform CSB incident on the tip of a circular cone. The waist is located directly at the tip. The Rayleigh length is  $b = 10 \Lambda$  ( $\Lambda =$  wavelength). The angle of incidence is  $\theta = 10^\circ$  of the vertical axis. The polarizations are as indicated.

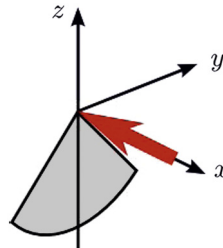


**Fig. 5.** Uniform CSB incident on the corner of a plane angular sector.

Note that we have to insert spherical Bessel functions of the first kind  $j_{\sigma\tau}$  ( $\tau \in \{s, h\}$ ) in all occurring vector spherical-multipole functions in case of a complex-source location  $\mathbf{r}_c$ .

## 5. Numerical results

First we have applied the described theory to the case of a uniform CSB which is incident directly towards the tip of a circular cone, i.e. an elliptic cone with  $k = 1$ . As has been shown in [9,10], in this case only the radial component of  $\mathbf{r}_c$ , that is  $r_c$  has to be chosen complex-valued while  $\vartheta_c$  and  $\varphi_c$  remain real-valued. Fig. 3 shows the total near field for a CSB which is incident from  $\theta = 10^\circ$  off the  $z$ -axis for the two indicated polarizations, whereas Fig. 4 represents the corresponding scattered far fields. We have obtained the scattered field by simply subtracting the incident from the total field. As a second example we have chosen a uniform CSB incident directly towards the corner of a plane angular sector described by  $\vartheta_0 = \pi$ , see Fig. 5. Again, we have chosen the waist to be located at the corner for achieving a plane-wave front at the area of interaction with the sector. Fig. 6 finally shows the scattered fields for different opening angles of the sector. We clearly observe that the interaction between the edges is dramatically increasing for smaller opening angles. Consequently, not just the area which is illuminated by the CSB contributes to the scattered field. Moreover, the characteristic structure of the scattered field extremely changes as a function of the opening angle.

Finally, it is important to note that all multipole expansions evaluated for these results show strong convergence. This is in contrast to the case of a full plane-wave incidence as treated in [11], where the obtained multipole series were non-convergent and special summation techniques had to be applied to come to meaningful results. The computational resources for evaluating the fields are in the range of CPU seconds on a standard personal computer.

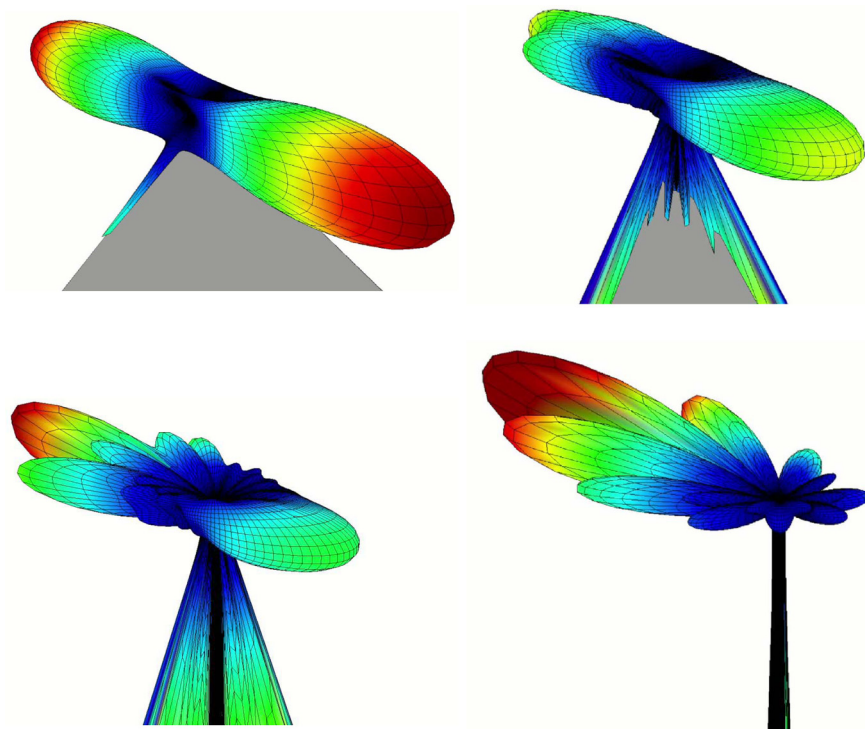


**Fig. 6.** Scattered field of a uniform CSB incident on the corner of a plane angular sector for different opening angles: Left upper  $90^\circ$ , right upper  $45^\circ$ , left lower  $25^\circ$ , right lower  $5^\circ$ . The waist is located directly at the corner of the sector. The Rayleigh length is  $b = 10 \Lambda$ . The electric field of the CSB is polarized in the  $y$ -direction, see Fig. 5.

## Acknowledgements

This work was supported by the Deutsche Forschungsgemeinschaft (DFG) under KL815/10-1&2.

## References

- [1] C.A. Balanis, *Advanced Engineering Electromagnetics*, John Wiley & Sons, 1989.
- [2] P. Moon, D.E. Spencer, *Field Theory Handbook*, 2nd ed., Springer Verlag, Berlin, Heidelberg, New York, 1971.
- [3] S. Blume, L. Klinkenbusch, Spherical-multipole analysis in electromagnetics, in: D.H. Werner, R. Mittra (Eds.), *Frontiers in Electromagnetics*, IEEE Press and Wiley, New York, 1999.
- [4] L.B. Felsen, Complex-source-point solutions of the field equations and their relation to the propagation and scattering of Gaussian beams, in: *Symposia Matematica*, vol. XVIII, Academic Press, London, 1976, pp. 40–56.
- [5] M. Couture, P.-A. Belanger, From Gaussian beam to complex-source-point spherical wave, *Phys. Rev. A* 24 (1981) 355–359.
- [6] L. Klinkenbusch, H. Brüns, Diffraction of a uniform complex-source beam by a circular cone, in: *Proc. 2014 International Conference on Electromagnetics in Advanced Applications, ICEAA14*, Palm Beach, Aruba, 2014, pp. 470–472.
- [7] A. Sommerfeld, *Lectures on Theoretical Physics, Part VI: Partial Differential Equations in Physics*, Harri Deutsch, Thun, Frankfurt/Main, Germany, 1978 (reprint of the 6th ed.; in German).
- [8] C.-T. Tai, *Dyadic Green's Functions in Electromagnetic Theory*, Scantron: Intext Educational Publishers, 1971.
- [9] H. Brüns, L. Klinkenbusch, Electromagnetic diffraction and scattering of a complex-source beam by a semi-infinite circular cone, *Adv. Radio Sci.* 11 (2013) 31–36, <http://dx.doi.org/10.5194/ars-11-31-2013>.
- [10] M. Katsav, E. Heyman, L. Klinkenbusch, Complex-source beam diffraction by an acoustically soft or hard circular cone, in: *Proc. 2012 International Conference on Electromagnetics in Advanced Applications, ICEAA12*, Cape Town, South Africa, 2012, pp. 135–138.
- [11] L. Klinkenbusch, Electromagnetic scattering by semi-infinite circular and elliptic cones, *Radio Sci.* 42 (2007) RS6510.